

## ARTICLES

# Geometric frustration in buckled colloidal monolayers

Yilong Han<sup>1,2\*</sup>, Yair Shokef<sup>1\*†</sup>, Ahmed M. Alsayed<sup>1</sup>, Peter Yunker<sup>1</sup>, Tom C. Lubensky<sup>1</sup> & Arjun G. Yodh<sup>1</sup>

**Geometric frustration arises when lattice structure prevents simultaneous minimization of local interaction energies. It leads to highly degenerate ground states and, subsequently, to complex phases of matter, such as water ice, spin ice, and frustrated magnetic materials. Here we report a simple geometrically frustrated system composed of closely packed colloidal spheres confined between parallel walls. Diameter-tunable microgel spheres are self-assembled into a buckled triangular lattice with either up or down displacements, analogous to an antiferromagnetic Ising model on a triangular lattice. Experiment and theory reveal single-particle dynamics governed by in-plane lattice distortions that partially relieve frustration and produce ground states with zigzagging stripes and subextensive entropy, rather than the more random configurations and extensive entropy of the antiferromagnetic Ising model. This tunable soft-matter system provides a means to directly visualize the dynamics of frustration, thermal excitations and defects.**

Geometric frustration arises in physical and biological systems<sup>1</sup> that range from water<sup>2</sup> and spin ice<sup>3</sup> to magnets<sup>4,5</sup>, ceramics<sup>6</sup> and high-transition-temperature superconductors<sup>7</sup>. The essence of this phenomenon is best captured in the model of Ising spins arranged on a two-dimensional (2D) triangular lattice and interacting antiferromagnetically<sup>8,9</sup>; two of the three spins on any triangular plaquette within this lattice can be antiparallel to minimize their antiferromagnetic interaction energy, but the third spin is frustrated because it cannot be simultaneously antiparallel to both neighbouring spins (Fig. 1a). Such frustration leads to materials with many degenerate ground states and extensive entropy proportional to the number of particles in the system. Consequently, small perturbations can

introduce giant fluctuations with peculiar dynamics. Traditionally, these phenomena have been explored in atomic materials by ensemble averaging techniques, such as neutron and X-ray scattering, muon spin rotation, nuclear magnetic resonance and measurements of heat capacity and susceptibility<sup>5</sup>. More recently, artificial arrays of mesoscopic constituents have been fabricated to probe geometric frustration at the single-‘particle’ level. Examples include Josephson junctions<sup>10</sup>, superconducting rings<sup>11</sup>, ferromagnetic islands<sup>12–14</sup> and recent simulations<sup>15</sup> of charged colloids in optical traps. But observations in these model systems have been limited to the static patterns into which these systems freeze when cooled. Thus many questions about frustrated systems remain unexplored, particularly those associated with single-particle dynamics. For example, how, when and why do individual particles change states to accommodate their local environments, and what kinetic mechanisms govern transitions to glassy phases?

Here we report the static and dynamic properties of a self-assembled colloidal system analogous to Wannier’s antiferromagnetic Ising model<sup>8</sup>. Densely packed spheres between parallel walls form an in-plane triangular lattice with out-of-plane up and down buckling<sup>16–26</sup>. The up–down states of the spheres produced by buckling are analogous to up–down states of Ising spins (Fig. 1b). Nearest-neighbour excluded volume interactions between particles favour opposite states for neighbouring particles, as do the antiferromagnetic interactions between neighbouring spins in the Ising model. In contrast to engineered mesoscopic systems<sup>10–14</sup>, however, our colloidal system facilitates easy tuning of the effective antiferromagnetic interaction through changes in the diameter of temperature-sensitive microgel spheres<sup>27</sup>. The colloidal system also permits direct visualization of thermal motion at the single-particle level. In the limit of weak confinement, or weak interaction strength, system properties closely follow those predicted for the antiferromagnetic Ising model, but in the limit of strong confinement, they do not. For strong interactions, the lattice deforms to maximize free volume, and the collective nature of the free-volume-dominated free energy characteristic of most soft-matter systems becomes important. We understand these effects

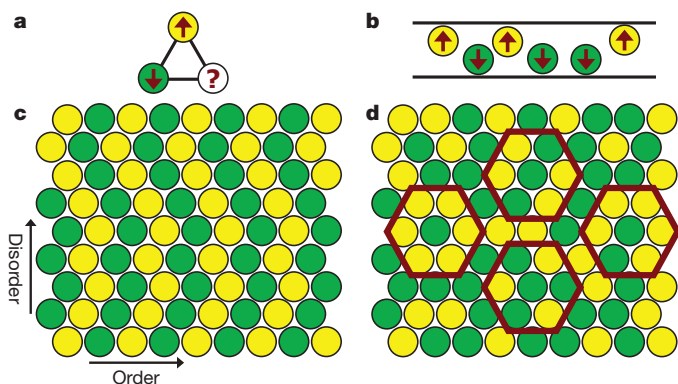


**Figure 1 | Ising ground state.** **a**, Three spins on a triangular plaquette cannot simultaneously satisfy all antiferromagnetic interactions. **b**, For colloids confined between walls separated by a distance of the order 1.5 sphere diameters (side view), particles move to opposite walls in order to maximize free volume. **c, d**, Ising ground-state configurations wherein each triangular plaquette has two satisfied bonds and one frustrated bond. **c**, Zigzag stripes generated by stacking rows of alternating up/down particles with random sidewise shifts; all particles have exactly 2 frustrated neighbours. **d**, Particles in disordered configurations have 0, 1, 2 or 3 frustrated neighbours (red hexagons).

<sup>1</sup>Department of Physics and Astronomy, University of Pennsylvania, 209 South 33rd Street, Philadelphia, Pennsylvania 19104, USA. <sup>2</sup>Department of Physics, Hong Kong University of Science and Technology, Clear Water Bay, Kowloon, Hong Kong. <sup>†</sup>Present address: Department of Physics of Complex Systems, Weizmann Institute of Science, Rehovot 76100, Israel. \*These authors contributed equally to this work.

theoretically in terms of tiling of the plane by isosceles triangles. The tiling scheme identifies a ground state consisting of zigzagging stripes with subextensive entropy. Interestingly, in contrast to Ising-model predictions, first measurements of single-particle ‘spin-flipping’ suggest that flipping dynamics depend not only on the number of nearest-neighbour frustrated ‘bonds’, but on how these bonds are arranged. Thus we begin to explore connections between frustrated soft matter and hard materials such as frustrated antiferromagnetic media. (Unless otherwise specified, we use ‘antiferromagnetic Ising model’ to refer to antiferromagnetic spins on a rigid triangular lattice; we will, however, also discuss this model on a deformable lattice.)

### Experimental system

For walls separated by distances of the order of 1.5 sphere diameters, the particles maintain in-plane triangular order but buckle out-of-plane (Fig. 2a, d). This buckling minimizes system free energy,  $F = U - TS$ , where  $U$  is internal energy,  $T$  temperature and  $S$  entropy. The bare interaction potential between our weakly charged<sup>27</sup> particles was measured to be short ranged and repulsive<sup>28</sup>, that is, nearly hard core. Thus the dominant contribution to the free energy is entropic. Spheres will move apart to minimize internal energy and to maximize their free volume and entropy resulting from it. This effect gives rise to multi-body effective interactions between spheres which, for low volume fractions, can be well approximated by a two-body repulsive entropic potential with range of the order of the interparticle spacing<sup>29</sup>. At high volume fraction, many-body contributions to the potential may become important. The effective repulsion causes spheres to move to the top or bottom wall, and nearest neighbours maximize free volume by moving to opposite walls (Fig. 1b). Buckled colloidal monolayers were first observed more than two decades ago<sup>16–18</sup>, and the antiferromagnetic analogy was then suggested<sup>17,30</sup> (note that ref. 30 includes the experimental work reported in ref. 16). However, to date, few quantitative measurements have been performed on this system class, and the themes explored by most early work centred on structural transitions exhibited by colloidal thin films as a function of increasing sample thickness<sup>17–20,22–24</sup>, rather than their connection to frustrated antiferromagnets. The use of temperature-sensitive diameter-tunable NIPA (N-isopropyl acrylamide) microgel spheres<sup>27</sup> also distinguishes our experiments from

earlier work. By varying temperature we change particle size and sample volume fraction and, therefore, vary the strength of the effective antiferromagnetic interparticle interactions.

Samples were prepared at low volume fraction near the melting point to produce 2D crystal domains with  $\sim 10^4$  spheres covering an area of the order of  $60 \mu\text{m}^2$ . Video microscopy measurements were carried out far from grain boundaries on an  $\sim 32 \mu\text{m}^2$  central area ( $\sim 2,600$  spheres) within the larger crystal domain. Particle motions were observed by microscope, recorded to videotape using a CCD camera and tracked by standard image-processing techniques<sup>31</sup>. In most colloid experiments, the important thermodynamic control variable is particle volume fraction. The present experiment achieved substantial variation in sphere diameter using small changes in temperature, which altered thermal energies by less than 1%. Here we monitor and report temperature rather than volume fraction because the interactions between spheres contain a soft ‘tail’ that introduces some ambiguity into the assignment of a geometric diameter to the particles. Below  $24^\circ\text{C}$ , the system is jammed and no dynamics are observed. Above  $27.5^\circ\text{C}$ , the in-plane crystals melt. Our primary measurements of the frustrated states probe five temperatures from  $24.7^\circ\text{C}$  to  $27.1^\circ\text{C}$  in  $0.6^\circ\text{C}$  steps. In this range, the hydrodynamic diameter of the nearly-density-matched particles decreases linearly with increasing temperature from  $0.89 \mu\text{m}$  to  $0.76 \mu\text{m}$  (see Supplementary Fig. 1), whereas the average in-plane particle separation remains constant (see Supplementary Table 1). The measured in-plane structures are crystalline. To reach thermal equilibration, the sample was annealed near the melting point before the temperature was slowly decreased. (Here ‘annealed’ means that the sample was left to evolve for several hours near the melting point to relieve possible unbalanced pressure and provide time for defects to move to produce higher quality crystals.) Slow cycling through this temperature range produced no hysteresis.

### Antiferromagnetic order

The images in Fig. 2a, d show roughly half of the spheres as bright because they are in the focal plane of the microscope; the other half, located near the bottom plate, are slightly out-of-focus and appear dark. A histogram, based on image brightness, showing the degree to which particles are ‘up’ or ‘down’ is given in Supplementary Fig. 2.

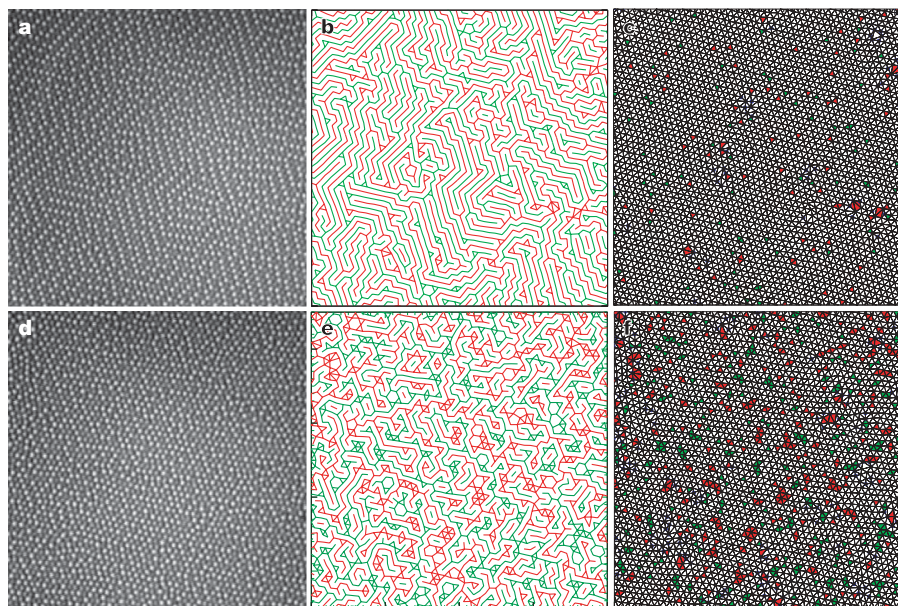


**Figure 2 | Buckled monolayer of colloidal spheres.** Shown are data from an area of  $32 \mu\text{m}^2$  at  $T = 24.7^\circ\text{C}$  (a–c) and  $27.1^\circ\text{C}$  (d–f). **a, d**, Bright spheres, up; dark spheres, down. **b, e**, Labyrinth patterns obtained by drawing only the frustrated up–up (red) and down–down (green) bonds. **c, f**, Corresponding Delaunay triangulations. Blue dots mark defects in the

triangular lattice, that is, particles that do not have exactly six nearest neighbours. Thermally excited triangles with three spheres up/down are labelled by red/green. These snapshots are taken from Supplementary Movies.

The histogram is bimodal, but clearly a range of ‘up’ and ‘down’ is evident in this classical system. The continuous brightness profile was discretized into two ‘Ising’ states with  $s_i = \pm 1$  (here  $s_i$  refers to the state of particle  $i$ ). The brightness cut-off was chosen near the interior minimum so that half the particles are up and half are down. Shifting this cut-off changed structural and dynamical analyses very little (that is, by a few per cent) for shifts of a few per cent in up/down cut-off. The nature of the frustrated states can be exhibited in different ways in processed images. One way focuses on the ‘bonds’ between particles. We refer to pairs of neighbouring particles ( $i$  and  $j$ ) in opposite states ( $s_i s_j = -1$ ) as satisfied bonds (that is, satisfying the effective antiferromagnetic interaction), and to up–up or down–down pairs (with  $s_i s_j = 1$ ) as frustrated bonds. Images show that the frustrated bonds form a nearly single-line labyrinth (Fig. 2b) at low temperature that then nucleates into domains (Fig. 2e) at high temperature. Local antiferromagnetic order is alternatively characterized by the average number of frustrated bonds per particle,  $\langle N_f \rangle$ . In the limit of weak interactions, an Ising system chooses a completely random configuration with half of the six bonds satisfied and half frustrated, leading to  $\langle N_f \rangle = 3$ . In the limit of strong interactions, on the other hand, each triangular plaquette has one frustrated bond (Fig. 1a), a third of the bonds are frustrated, and  $\langle N_f \rangle = 2$ .  $\langle N_f \rangle$  is a linear rescaling of the density of excited triangles (3 up or 3 down) in Fig. 2c,  $f$ , which ranges from 0 in the Ising ground state to 0.5 for a random configuration. We find that  $\langle N_f \rangle$  decreased from approximately 2.5 to 2.1 in the temperature interval 27.1–24.7 °C. Detailed statistics of the different local configurations are presented in Supplementary Table 1.

We first consider the static properties of the frustrated samples. In particular, we aim to identify similarities and differences between the colloidal system and the Ising model. As the temperature is lowered to increase particle diameter,  $\langle N_f \rangle$  is observed to approach 2. This behaviour is expected in the Ising-model ground state. However, the vast majority of Ising ground-state configurations are disordered. The colloidal monolayers, by contrast, condense into stripe phases. The stripes are not straight, as could be produced by higher-order interparticle interactions<sup>32</sup>. Rather, they bend and form zigzag patterns<sup>22–26</sup> (see Fig. 2a and configuration statistics in Supplementary Table 1). In this colloidal zigzag-stripped phase, we measured spatial correlations  $I(i-j) = [\langle s_i s_j \rangle - \langle s \rangle^2] / [\langle s^2 \rangle - \langle s \rangle^2]$  over separations  $|i-j|$ , along the principal lattice directions, of up to 20 particles, and found that they decay exponentially in magnitude with alternating sign (Supplementary Fig. 4).  $I(i-j)$  is positive for  $i-j$  even and negative for  $i-j$  odd. In contrast,  $I(i-j)$  averaged over the Ising ground state is positive when  $i-j$  is an integer multiple of 3. Furthermore, for zigzagging stripes each particle has exactly two frustrated neighbours (Fig. 1c), whereas in the fully disordered Ising ground state  $N_f$  can be 0, 1, 2 or 3 (Fig. 1d) and only the average  $\langle N_f \rangle$  is 2. These observations suggest that fluctuations in  $N_f$ , that is,  $\text{Var}(N_f) = \langle N_f^2 \rangle - \langle N_f \rangle^2$ , might be a useful measure for distinguishing the zigzag-stripe phase observed here from the disordered Ising ground state. Figure 3 plots the behaviour of  $\text{Var}(N_f)$  as a function of  $\langle N_f \rangle$  for the Ising model and for data obtained both from experiments and from hard-sphere Monte Carlo simulations (see Supplementary Information). Results from experiment and simulation agree at both low and high volume fraction and differ from those of the Ising model, especially at high volume fraction when interactions are strong. Three length scales affect the physics in this problem: sphere diameter, wall separation, and lattice constant. Therefore, two length ratios can be varied. The simulations showed explicitly (Fig. 3, Supplementary Fig. 5) that the frustration behaviours as functions of sphere diameter for different plate separations were similar as long as the plate separation did not exceed approximately two particle diameters<sup>22,23</sup>.

### Zigzagging stripes

Ideal geometrically frustrated systems, such as the antiferromagnetic Ising model, are highly degenerate with extensive entropy at zero

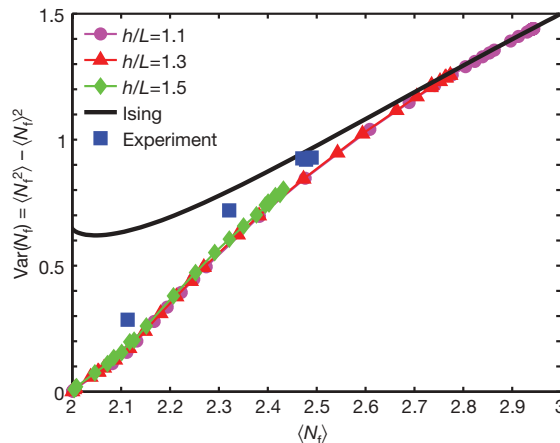


**Figure 3 | Fluctuation in the number of frustrated bonds per particle as a function of its average.** Experiments quantitatively agree with hard-sphere simulations at different plate separations,  $h$ , normalized by the average in-plane lattice constant,  $L$ . Simulations collapse onto a single curve and deviate significantly from the behaviour in the Ising model.

temperature. However, in real materials, subtle effects—for example anisotropic interactions<sup>9</sup>, long-range interactions<sup>32</sup>, boundary conditions<sup>33</sup> and lattice distortions<sup>34–36</sup>—relieve frustration. Our partially ordered zigzag-stripe phase at high volume fraction is an example of frustration relief by lattice distortion. In the colloidal monolayer the triangular packing is self-assembled, and the particles are not forced to remain at fixed positions on the lattice<sup>26</sup>. This deformability and the fact that the free volume of the system is a collective function of all particle positions breaks the mapping to simple Ising models with pair-wise-additive nearest-neighbour interactions. In fact, the positions of the colloidal particles may be thought of as comprising a planar structure that crumples between the two confining planes. This ‘crumpling’ leads to deformations of the planar triangular lattice with satisfied bonds (projected onto the plane) on average 3–4% shorter than frustrated bonds (see Supplementary Table 1). This difference is consistent with the notion that each pair of neighbouring particles prefers to be separated by the same fixed distance in three dimensions (3D), whether or not their connecting bond is satisfied.

A simple tiling argument demonstrates why the colloidal system ground-state configurations of stripes and zigzags pack better than the disordered Ising configurations (Fig. 4). The tiling model shows explicitly that maximal volume fractions of stripe and zigzag phases are the same (see Supplementary Information). Each triangular plaquette in the Ising ground state contains two satisfied bonds and one frustrated bond. Thus, when spheres are close-packed in 3D, the equilateral triangle defined by each such triplet of neighbouring particles is tilted, and when projected onto the 2D plane, it deforms into an isosceles triangle with two short sides along the satisfied bonds and one long side along the frustrated bond (Fig. 4a, b). Subsequently, close-packed configurations of the buckled spheres in 3D are described by tilings of the plane by isosceles triangles. Figure 4c shows the configurations of isosceles triangles for different numbers of frustrated bonds ( $N_f$ ) in the basic hexagonal cell. By summing up the angles around the central vertex, one immediately sees that for  $N_f = 0, 1, 3$ , the triangles cannot close-pack. Only the two configurations with  $N_f = 2$  enable tiling the plane with isosceles triangles, or, equivalently, close-packing of the buckled spheres in 3D. Configuration 2b corresponds to a bend in a stripe, and 2c to a stripe continuing along a straight line. Both have the same maximal volume fraction, thus corroborating observations of zigzagging stripes in the experiments and simulations.

Experiments and simulations suggest a possible preference for the stripes to form straight segments rather than to bend easily and thus to generate randomly zigzagging configurations (Fig. 2a). Zigzagging

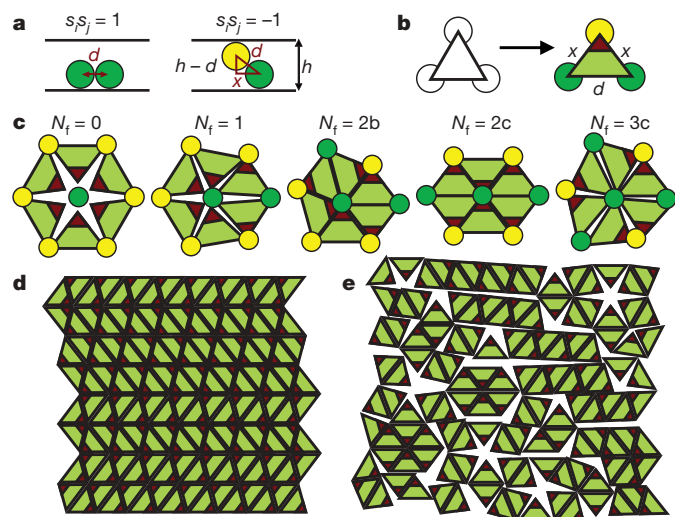


**Figure 4 | Tiling the plane with isosceles triangles.** **a**, Close-packed spheres are separated by one particle diameter  $d$  in 3D. This distance projected on the 2D plane remains  $d$  for a frustrated bond ( $s_i s_j = 1$ ), but is reduced to  $x = \sqrt{d^2 - (h-d)^2}$  for a satisfied bond ( $s_i s_j = -1$ ). **b**, Viewed from above, each plaquette in the lattice tends to deform to an isosceles triangle with one long side ( $d$ ) along the frustrated bond and two short sides ( $x < d$ ) along the satisfied bonds. The angle larger than  $\pi/3$  is marked in red. **c**, All possible in-plane local particle configurations appearing in the Ising ground state. The isosceles triangles can tile the plane without extra space only for  $N_f = 2$ . The ‘white space’ for  $N_f = 0, 1, 3$  corresponds to additional excluded volume. **d, e**, Tilings corresponding to striped and disordered Ising ground-state configurations, respectively, of Fig. 1c, d.

stripes can be viewed as a random stack of ordered lines of alternating up and down particles (Fig. 1c); thus straight and zigzagging stripes are analogous to the face-centred cubic (f.c.c.) lattice and the random hexagonal-close-packed (r.h.c.p.) structure<sup>20</sup> in 3D. Straight and zigzagging stripes have the same maximal volume fraction in the close-packed limit. However, for smaller volume fractions there may be an order-by-disorder effect<sup>5,37</sup>, giving a small free volume advantage of straight stripes over zigzagging ones, similar to the free volume advantage<sup>38</sup> of f.c.c. over r.h.c.p. in 3D. Indeed, stripes in Fig. 2a persist in the same direction for several particle diameters and the same appears more ordered than the random zigzag stripes of Fig. 1c.

Instead of an extensive entropy at zero temperature<sup>8</sup>, wherein  $S$  scales linearly with the number of particles in the system ( $N$ ), the buckled system has subextensive entropy. The number of zigzagging striped configurations grows exponentially with the linear dimension of the system (there are two possible ways of placing one row relative to its predecessor in Fig. 1c); hence the entropy scales<sup>39</sup> as  $\sqrt{N}$ . Alternatively, a non-branching single-line labyrinth is dictated by  $\sim \sqrt{N}$  particles on the boundary, and a cluster of order  $\sqrt{N}$  particles should be flipped for the system to rearrange from one zigzag-stripe configuration to another. Subextensive ground-state entropy also appears in related models emulating systems with glassy dynamics<sup>40</sup>. Similar zigzag stripes have been observed in superconducting arrays in external fields<sup>41</sup> and in microscopic Ising models<sup>42</sup>.

### Dynamics

Taken together, these observations have interesting consequences for the ground-state dynamics of frustrated systems. The Ising ground state has a local zero-energy mode, as shown in configuration 3c in Fig. 5a: the central particle can flip without changing the energy of the system, thus rapidly relaxing spin correlations via a sequence of such single spin flips, even at zero temperature. For buckled spheres, on the other hand, the close-packed configurations have only particles with  $N_f = 2$ , and, moreover, even a particle with  $N_f = 3$  in an excited configuration has to cross an energy barrier in order to flip. Thus frustration relief creates a ‘glass-like’ medium having energy barriers

between the various energy minima. Like the glassy behaviour of an Ising model on a deformable lattice<sup>43,44</sup>, the slow dynamics we observe at low temperature is a consequence of the absence of local zero-energy modes in the bulk.

Our system permits direct visualization of ‘spin flipping’ and the motions of thermal excitations and defects in frustrated systems (see Supplementary Movies). Thermal excitations labelled as coloured triangles in Fig. 2c, f were typically found to be generated/annihilated in pairs owing to the flipping of a particle shared by the two triangles. Well-isolated thermal excitations, on the other hand, appear to be more stable. To quantify these effects, we first extract the full time trajectory,  $s_i(t)$ , of each particle  $i$  from the movies. In Fig. 5b we plot the single-particle autocorrelation function  $C(t) = [\langle s_i(t)s_i(0) \rangle - \langle s_i \rangle^2] / [\langle s_i^2 \rangle - \langle s_i \rangle^2]$ , averaged over all particles not at lattice defects. As the temperature is lowered, the correlation function develops a stretched exponential form,  $C(t) = \exp[-(t/\tau)^\beta]$ . The measured relaxation time  $\tau$  exhibits a dramatic increase as the particles swell at low temperature, whereas the extracted stretching exponent  $\beta$  decreases, indicating slow dynamics similar to those found in glasses<sup>45</sup>.

To further explore the dynamics of different local configurations (defined in Fig. 5a), Fig. 5c shows the measured flipping rate  $f_i$  of

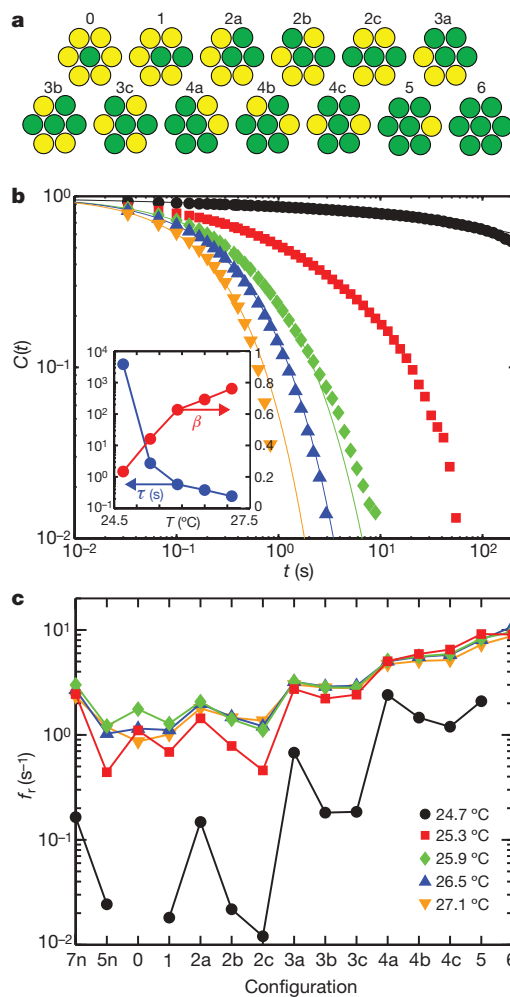


**Figure 5 | Single-particle dynamics.** **a**, Local configurations are labelled by their value of  $N_f$  and an index a, b, c indicating the precise geometrical arrangement of the frustrated neighbours for  $N_f = 2, 3, 4$ . Symmetry under rotation and inversion reduces the  $2^7$  possible configurations to the 13 given here. **b**, Single-particle autocorrelation functions plotted versus decay time. Lines are fits to stretched exponentials  $C(t) = \exp[-(t/\tau)^\beta]$ , with  $\tau$  and  $\beta$  given in the inset. **c**, Flipping rates for the different local environments. Configurations 7n and 5n are defects in the in-plane lattice, with 7 and 5 nearest neighbours.

single particles with a fixed neighbour structure. We measured the probability  $p$  that a particle flips between consecutive images given that the Ising states of its neighbours remained unchanged. The time intervals of  $dt = 1/30$  s between frames were short enough that  $p$  was typically small (0.36 at most) and the flip rate could be approximated by  $f_r = p/dt$ . At high temperature, the behaviour is similar to that of an Ising model undergoing Glauber dynamics:  $f_r \propto \exp(-\Delta E/k_B T)$ , where the energy difference  $\Delta E$  is proportional to the difference in  $N_f$  before and after flipping. As the volume fraction is increased by lowering the temperature, particle dynamics slow by 1–2 orders of magnitude and, more interestingly, significant differences develop between different geometrical configurations with the same  $N_f$ . Such phenomena may not appear in the simple Ising model where the Hamiltonian depends only on  $N_f$ .

Defects in the underlying lattice can strongly affect the properties of frustrated systems. However, detailed knowledge about the role of defects in frustrated systems is very limited. Our experiments permit direct visualization of defects nucleating, annihilating and diffusing (Supplementary Movies). By comparing trajectories containing different numbers and types of defects, initial studies suggest that defects, namely particles that do not have exactly six nearest neighbours, have enhanced in-plane diffusion (Supplementary Fig. 6) and slower flipping dynamics than those averaged over particles with six nearest neighbours.

## Outlook

We have presented experimental measurements of single-particle statics and dynamics in a geometrically frustrated system. Other experimental systems offering ‘single-spin’ resolution are based on lithography<sup>10–12</sup>. An attractive feature of the lithographic systems is that any underlying lattice can be created. Colloidal suspensions in 2D, by contrast, will self-assemble into triangular lattices unless an external potential is applied, and because the colloidal system is entirely self-assembling, it possesses a comparatively rich phenomenology originating from lattice deformability. The colloids also offer the possibility of dynamical studies; the lithography-based arrays, by contrast, are frozen in place.

The 2D colloidal frustrated ‘antiferromagnet’ we have studied provides an ideal platform for future study of the properties of frustrated and glassy systems. Sample dynamics and structure can be microscopically imaged, and the system can be perturbed and manipulated with laser tweezers and other tools. It thus offers hope for deeper insights into the interplay between frustration relaxation and order—for example the formation of phases with lower entropy than the antiferromagnetic Ising ground state—and into the connections between glassy dynamics, frustration and subextensive yet system-size-divergent entropy. Further experiments to address these issues are readily envisaged. For example, potential energy landscapes for the particles can be created using laser tweezers of varying periodicity and strength (including rigid lattices), enabling experimenters to explore the role of lattice deformability in the dynamics and the creation of structure. Optical or magnetic traps can be used to flip and to move individual spins, and video microscopy can be used to probe the resulting system’s responses. Boundaries affect frustration, but they are not well studied; such effects could be created by changing sample cell geometry or by fixing particles to the boundary. Gravity, external fields, and surface treatment can be used to mimic the effects of applied magnetic fields on frustrated magnetic systems. Defects affect frustration but have not been explored at the single-particle level; such effects can be studied by doping with particles having different shapes and interaction potentials. In the theoretical arena, it will be interesting to consider possible modifications to the rigid-lattice Ising model that generate a zigzagged-stripe ground state. This should allow a fuller exploration of the relation between buckled colloidal systems and the compressible Ising model, including the possibility of generating order-by-disorder via thermal fluctuations. It should also

enable the study of glassy dynamics arising from subextensive zero-temperature entropy.

*Note added in proof:* Blunt *et al.*<sup>46</sup> have recently measured motions of excitations in a molecular system which may be mapped onto the triangular-lattice antiferromagnetic Ising model.

Received 11 July; accepted 21 October 2008.

- Moessner, R. & Ramirez, A. R. Geometrical frustration. *Phys. Today* **59**, 24–26 (2006).
- Pauling, L. The structure and entropy of ice and of other crystals with some randomness of atomic arrangement. *J. Am. Chem. Soc.* **57**, 2680–2684 (1935).
- Harris, M. J., Bramwell, S. T., McMorrow, D. F., Zeiske, T. & Godfrey, K. W. Geometrical frustration in the ferromagnetic pyrochlore  $\text{Ho}_2\text{Ti}_2\text{O}_7$ . *Phys. Rev. Lett.* **79**, 2554–2557 (1997).
- Bramwell, S. T. & Gingras, M. J. P. Spin ice state in frustrated magnetic pyrochlore materials. *Science* **294**, 1495–1501 (2001).
- Moessner, R. Magnets with strong geometric frustration. *Can. J. Phys.* **79**, 1283–1294 (2001).
- Ramirez, A. R. Geometric frustration: Magic moments. *Nature* **421**, 483 (2003).
- Anderson, P. W. The resonating valence bond state in  $\text{La}_2\text{CuO}_4$  and superconductivity. *Science* **235**, 1196–1198 (1987).
- Wannier, G. H. Antiferromagnetism. The triangular Ising net. *Phys. Rev.* **79**, 357–364 (1950); erratum *Phys. Rev. B* **7**, 5017 (1973).
- Houtappel, R. M. F. Order-disorder in hexagonal lattices. *Physica* **16**, 425–455 (1950).
- Davidović, D. *et al.* Correlations and disorder in arrays of magnetically coupled superconducting rings. *Phys. Rev. Lett.* **76**, 815–818 (1996).
- Hilgenkamp, H. *et al.* Ordering and manipulation of the magnetic moments in large-scale superconducting  $\pi$ -loop arrays. *Nature* **422**, 50–53 (2003).
- Wang, R. F. *et al.* Artificial ‘spin ice’ in a geometrically frustrated lattice of nanoscale ferromagnetic islands. *Nature* **439**, 303–306 (2006).
- Möller, G. & Moessner, R. Artificial square ice and related dipolar nanoarrays. *Phys. Rev. Lett.* **96**, 237202 (2006).
- Nisoli, C. *et al.* Ground state lost but degeneracy found: The effective thermodynamics of artificial spin ice. *Phys. Rev. Lett.* **98**, 217203 (2007).
- Libál, A., Reichhardt, C. & Reichhardt, C. J. O. Realizing colloidal artificial ice on arrays of optical traps. *Phys. Rev. Lett.* **97**, 228302 (2006).
- Koshikiya, Y. & Hachisu, S. [in Japanese] *Lecture at Colloid Symposium of Japan* (1982).
- Pieranski, P., Strzelecki, L. & Pansu, B. Thin colloidal crystals. *Phys. Rev. Lett.* **50**, 900–903 (1983).
- Van Winkle, D. H. & Murray, C. A. Experimental observation of two-stage melting in a classical two-dimensional screened Coulomb system. *Phys. Rev. Lett.* **58**, 1200–1203 (1987).
- Weiss, J. A., Oxtoby, D. W., Grier, D. G. & Murray, C. A. Martensitic transition in a confined colloidal suspension. *J. Chem. Phys.* **103**, 1180–1190 (1995).
- Pansu, B., Pieranski, P., & Pieranski, P. Direct observation of a buckling transition during the formation of thin colloidal crystals. *J. Phys.* **45**, 331–339 (1984).
- Chou, T. & Nelson, D. R. Buckling instabilities of a confined colloid crystal layer. *Phys. Rev. E* **48**, 4611–4621 (1993).
- Schmidt, M. & Löwen, H. Freezing between two and three dimensions. *Phys. Rev. Lett.* **76**, 4552–4555 (1996).
- Schmidt, M. & Löwen, H. Phase diagram of hard spheres confined between two parallel plates. *Phys. Rev. E* **55**, 7228–7241 (1997).
- Zangi, R. & Rice, S. A. Phase transitions in a quasi-two-dimensional system. *Phys. Rev. E* **58**, 7529–7544 (1998).
- Melby, P. *et al.* The dynamics of thin vibrated granular layers. *J. Phys. Condens. Matter* **17**, S2689–S2704 (2005).
- Osterman, N., Babič, D., Poberaj, I., Dobnikar, J. & Zihlerl, P. Observation of condensed phases of quasiplanar core-softened colloids. *Phys. Rev. Lett.* **99**, 248301 (2007).
- Alsayed, A. M., Islam, M. F., Zhang, J., Collings, P. J. & Yodh, A. G. Premelting at defects within bulk colloidal crystals. *Science* **309**, 1207–1210 (2005).
- Han, Y., Ha, N. Y., Alsayed, A. M. & Yodh, A. G. Melting of two-dimensional tunable-diameter colloidal crystals. *Phys. Rev. E* **77**, 041406 (2008).
- Shokef, Y. & Lubensky, T. C. Stripes, zigzags, and slow dynamics in buckled hard spheres. Preprint at (<http://arxiv.org/abs/0807.4884>) (2008).
- Ogawa, T. A maze-like pattern in a monodisperse latex system and the frustration problem. *J. Phys. Soc. Jpn* **52** (Suppl.), 167–170 (1983).
- Crocker, J. C. & Grier, D. G. Methods of digital video microscopy for colloidal studies. *J. Colloid Interface Sci.* **179**, 298–310 (1996).
- Metcalf, B. D. Ground state spin orderings of the triangular Ising model with the nearest and next nearest neighbor interaction. *Phys. Lett. A* **46**, 325–326 (1974).
- Millane, R. P. & Blakeley, N. D. Boundary conditions and variable ground state entropy for the antiferromagnetic Ising model on a triangular lattice. *Phys. Rev. E* **70**, 057101 (2004).
- Chen, Z. Y. & Kardar, M. Elastic antiferromagnets on a triangular lattice. *J. Phys. C* **19**, 6825–6831 (1986).
- Gu, L., Chakraborty, B., Garrido, P. L., Phani, M. & Lebowitz, J. L. Monte Carlo study of a compressible Ising antiferromagnet on a triangular lattice. *Phys. Rev. B* **53**, 11985–11992 (1996).

36. Lee, S.-H., Broholm, C., Kim, T. H., Ratcliff, W. & Cheong, S.-W. Local spin resonance and spin-Peierls-like phase transition in a geometrically frustrated antiferromagnet. *Phys. Rev. Lett.* **84**, 3718–3721 (2000).
37. Villain, J., Bidaux, R., Carton, J. P. & Conte, R. Order as an effect of disorder. *J. Phys.* **41**, 1263–1272 (1980).
38. Mau, S. C. & Huse, D. A. Stacking entropy of hard-sphere crystals. *Phys. Rev. E* **59**, 4396–4401 (1999).
39. Liebmann, R. *Statistical Mechanics of Periodic Frustrated Ising Systems* (Springer, 1986).
40. Nussinov, Z. Avoided phase transitions and glassy dynamics in geometrically frustrated systems and non-Abelian theories. *Phys. Rev. B* **69**, 014208 (2004).
41. Shih, W. Y. & Stroud, D. Two-dimensional superconducting arrays in a magnetic field: Effects of lattice structures. *Phys. Rev. B* **32**, 158–165 (1985).
42. Nussinov, Z. Commensurate and incommensurate O(n) spin systems: novel even-odd effects, a generalized Mermin-Wagner-Coleman theorem, and ground states. Preprint at (<http://arxiv.org/abs/cond-mat/0105253>) (2001).
43. Chakraborty, B., Gu, L. & Yin, H. Glassy dynamics in a frustrated spin system: The role of defects. *J. Phys. Condens. Matter* **12**, 6487–6495 (2000).
44. Yin, H. & Chakraborty, B. Entropy-vanishing transition and glassy dynamics in frustrated spins. *Phys. Rev. Lett.* **86**, 2058–2061 (2001).
45. Ediger, M. D. Spatially heterogeneous dynamics in supercooled liquids. *Annu. Rev. Phys. Chem.* **51**, 99–128 (2000).
46. Blunt, M. O. *et al.* Random tiling and topological defects in a two-dimensional molecular network. *Science* **322**, 1077–1081 (2008).

**Supplementary Information** is linked to the online version of the paper at [www.nature.com/nature](http://www.nature.com/nature).

**Acknowledgements** We thank B. Chakraborty, R. D. Kamien, D. Li, A. J. Liu, C. D. Modes, T.-K. Ng, S. A. Rice, Y. Snir, T. A. Witten and Y. Zhou for discussions. This work was supported primarily by the NSF through MRSEC grant DMR-0520020 and partially by DMR-0804881 (NSF) and by NAG-2939 (NASA).

**Author Contributions** Y.H. and A.M.A. initialized the project. A.M.A. synthesized the particles. Y.H. conducted the experiments. Y.S. performed the simulations and provided the tiling model. Y.H. and Y.S. analysed and explained the experimental data. P.Y. characterized the particles. T.C.L. provided theoretical guidance. A.G.Y. provided experimental guidance. Y.H., Y.S., T.C.L. and A.G.Y. wrote the paper.

**Author Information** Reprints and permissions information is available at [www.nature.com/reprints](http://www.nature.com/reprints). Correspondence and requests for materials should be addressed to Y.S. ([yair.shokef@weizmann.ac.il](mailto:yair.shokef@weizmann.ac.il)) or Y.H. ([yilong@ust.hk](mailto:yilong@ust.hk)).